



POLITECNICO
MILANO 1863

SCUOLA DI INGEGNERIA INDUSTRIALE
E DELL'INFORMAZIONE

Reactivity Analysis for NUWARD Small Modular Reactor

LABORATORIO INGEGNERIA NUCLEARE
ENERGY ENGINEERING - NUCLEAR TRACK

Author: **Patrik Shytaj | Daniele Timpano | Carola Villa**

Student ID: 937044 | 934693 | 933658

Advisor: Prof. Stefano Lorenzi

Co-advisors:

Academic Year: 2021-2022

Abstract

Based on the NUWARD reactor design, this study assesses the prospect of **avoiding the use of soluble boron** in integral Pressurized Water Reactors (iPWRs). Soluble boron requires large recycling systems, and may lead to boron dilution accidents; hence new small modular reactor designs have been striving for alternative reactivity control solutions that may require significant changes in the original core.

Following the ideas suggested in the optimization of FLEXBLUE's core design, the working group focused on **the role of poisoned rods**, striving for the optimisation of the number of poisoned rods in the fuel assembly, their position and the quantity of Gd_2O_3 in each rod. Each of these design choice proves strictly interconnected with **uranium enrichment, cut-off burnup and refuelling strategies**.

Downstream of finding the best alternative that guarantees a good reactivity margin during all the fuel's lifetime and a reasonable burnup, the group made a study of the reactor's intrinsic stability by computing some **reactivity coefficients** such as the fuel temperature coefficient, moderator temperature coefficient, power coefficient and void coefficient. Lastly, the **operational stability** of the reactor has been studied by analyzing the worth of the control rods and the axial offset of power.

ACKNOWLEDGEMENTS: we would like to warmly thank our supervisor Professor Stefano Lorenzi for the invaluable help given during the analysis of the simulation results and crafting of the whole research work.

Keywords: Boron free, Reactivity margin, Burnup, Reactivity coefficients

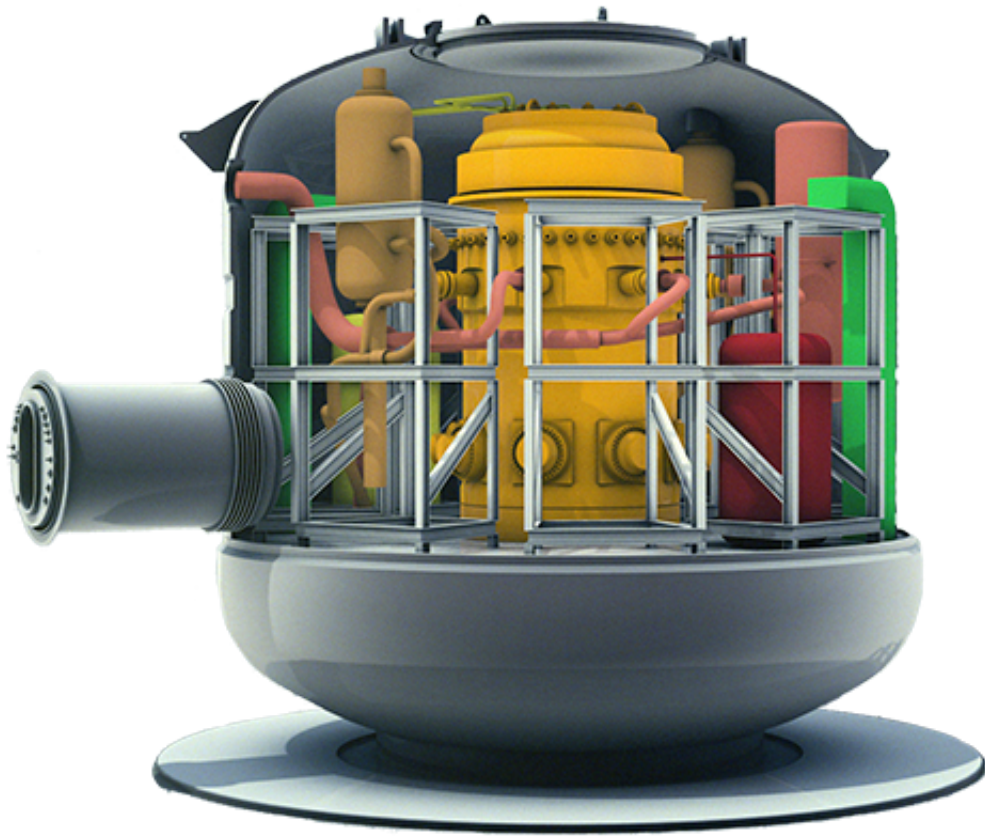


Figure 1: NUWARD reactor - section view

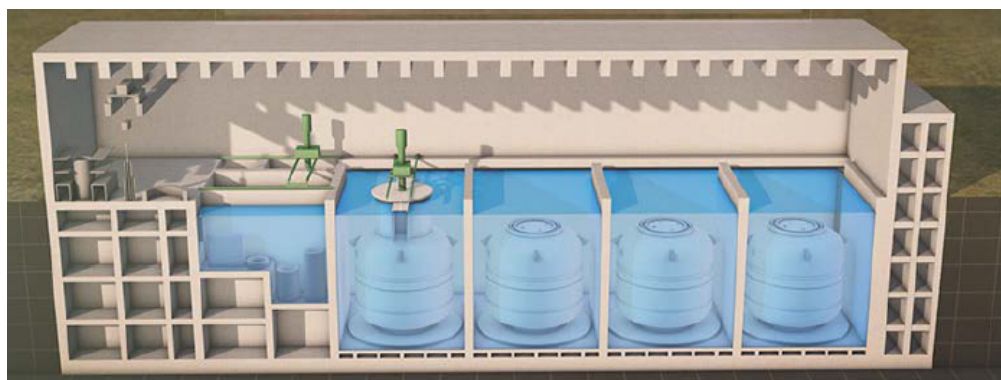


Figure 2: NUWARD reactor - power plant

Contents

Abstract	i
Contents	iii
1 Introduction	1
1.1 NUWARD - Small Modular Reactor	2
1.2 Numerical methods for neutronic analysis	4
2 Reactivity Analysis	5
2.1 Moderator to fuel ratio	5
2.2 Optimal enrichment and gadolinium	7
2.3 Selection of the best assembly geometry	11
3 Characterisation of fuel performance coefficients	15
3.1 Temperature Coefficients	15
3.1.1 Fuel Temperature Coefficient	16
3.1.2 Moderator Temperature Coefficient	17
3.2 Power Coefficient	19
3.3 Void Coefficient	21
4 Reactivity Control	25
5 Future developments	31
Bibliography	33
A Appendix A	35

List of Figures	43
------------------------	-----------

List of Tables	45
-----------------------	-----------

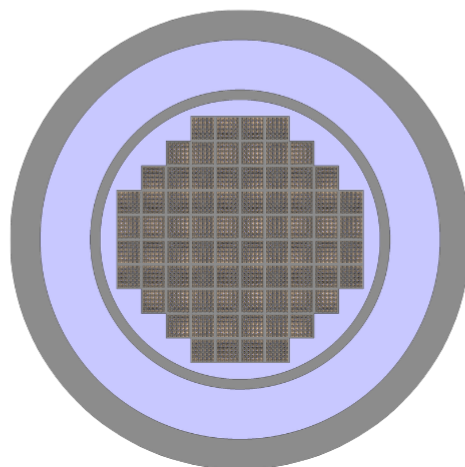
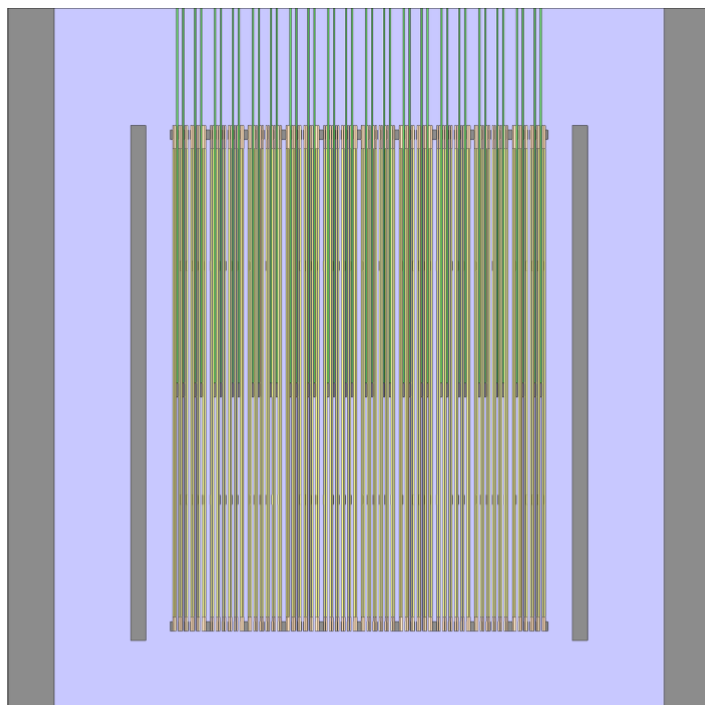


Figure 3: iPWR Model - Serpent Plot

1 | Introduction

The development of nuclear technologies for power generation world-wide has been moving towards a three-pronged strategy:

- the development of **Generation IV reactors** as stated in the framework of the Generation IV International Forum;
- the development of **Small Modular Reactors** aiming at enhanced safety features and the exploitation of the economy of multiples;
- the **enlargement and consolidation of the Gen III + reactors fleet** both in Europe and in the USA, with projects such as the AP1000 and the EPR2 [1];

In light of these development efforts, the two main drivers for the success of new-born nuclear power plants are **high burn-ups** and **higher efficiencies**. The focus on fuel features is an essential driver both for the assessment of NPP performance and for the fulfillment of safety standards and market expectations. Within this line of thoughts, the European Commission Taxonomy and the EU Green Deal have remarked the importance of accident tolerant fuels (ATF) [2] for the future of this energy source.

The project work for the Nuclear Engineering Laboratory strives for assessing **reactivity control** in a boron-free reactor design, investigating the effect on the fuel behaviour of differential enrichment (%wt of U^{235}), different core geometries, differential gadolinium concentrations in poisoned rods and their possible distributions in the core. Fuel characterisation has also been carried out by means of fuel performance coefficients.

We decided to focus on **NUWARD reactor** since it represents one of the most promising designs for integral Pressurised Water Reactor in the current worldwide scenario.

1.1. NUWARD - Small Modular Reactor

Nuward is a 340 MW_e power plant including two reactors in a single nuclear building [3]. It consists in an innovative design with the most compact reactor in the world, noticeably simplified by modularisation and system integration [4].

Table 1.1: NUWARD - General Overview

Design organisation	CEA EDF Naval Group and Technicatome
Coolant	Light Water
Moderator	Light Water
Design status	Conceptual Design
Country	France
Type	PWR
Purpose	Commercial

Table 1.2: NUWARD - Reactor Data

Neutron spectrum	Thermal
Reactor Thermal Output (MW _{th})	540
Power plant output gross (MW _e)	185
Power plant output net (MW _e)	170
Plant efficiency net (%)	31
Thermodynamic cycle	Rankine
Non-electrical applications	Optional

The Nuward reactor is a fully integrated PWR housing all the main cooling and control systems, including the control rod drive mechanisms (CRDM) inside the reactor pressure vessel. An integral reactor is a nuclear reactor design where all the significant primary components are contained inside the same vessel. This idea can be applied to any sort of underlying reactor design.

Even if integral reactors and SMRs are enjoying great success in recent years, this is not totally a “brand new” concept: the first iPWR dates back to nearly the start of commercial nuclear energy. During the 1950s, one of the promises that nuclear energy seemed to confer, at least so far for ships, was a compactness not equaled by conventional oil-fired boilers or diesel engines. The first iPWR was constructed in Germany as nuclear

steam supply for a ship, named Otto Hahn ship (the reactor was first started up in 1968, and had an operational period of 10 years).

Nuward design, as an integral reactor, presents several innovations compared to a standard PWR:

- Adoption of Passive Safety Systems
- Compactness of Containment and design simplification
- Modularisation and Multiple units

Safety

Nuward's design includes technical options aiming to reach and maintain a safe state for a long period (more than three days) without external resource, boron injections, electrical power supply and operator's action.

Enhanced safety features include the objective to reduce leakage, eliminate large break LOCA by design and limit the maximum Loss of Coolant Accident, adopting internal pipings with a diameter of less than 30 mm, directly connected to the Reactor Pressure Vessel and an integral and compact cooling system based on a once-through steam generator.

A large primary inventory, provides more time to actuate any regulation or automatic action in case of incidental power transients; Internal CRDMs system prevents from rod-ejection accidents, while the metallic submerged containment provides passive cooling for several days transferring the decay heat from the core to the water surrounding the containment using natural circulation.

Compactness and Boron Free design

Nuward design also aims to eliminate boron as a reactivity control method, so to avoid boron induced incidents and boron dilution that may occur during refuelling phase, accidental situations or shutdown.

Boron-related issues include primary corrosion due to boric acid, boron dilution accidents and increase of the Moderator Temperature Coefficient (MTC) [5]. The choice to opt for a soluble boron-free core is also widely justified by the voluminous recycling systems, which require frequent maintenance and are not suitable for the limited space

available in a integral reactor.

However, operating without soluble boron involves some challenges and problems; the presence of boron, homogeneously distributed in the coolant (which is very common in large PWRs), could be essential for several purposes:

- this soluble poison is necessary to provide sufficient negative reactivity to achieve cold shutdown, to mitigate the high reactivity of fresh fuel and to control the reactivity during the fuel depletion;
- moreover boron is also a convenient manner to quickly react to reactivity changes, such as during xenon transient, and to homogenize the power distribution in order to reduce the power peak [5].

Modularisation and multiple units

As a typical integral reactor, Nuward construction process is based on modularisation, staggered deployment, serial production and multi-units on the same site in order to reduce construction time and costs and to limit financial risk [6].

1.2. Numerical methods for neutronic analysis

In order to make calculations on the reactor, instead of solving the neutron transport equation, the selected method is to use a **Monte Carlo code**, the chosen one is **Serpent**. This approach reproduces, with a controllable statistical error, the physics of the reactor by simulating the random behaviour of a large number of neutrons and then collecting information about the interactions. To make a more accurate evaluation the same process is simulated by **Serpent** a sufficient number of times, called cycles, in each of them the neutrons start their lives and have random interactions with matter until all of them reach the end of their history, so the cycle ends and a new cycle starts [7].

For the calculations the set parameters were **10 000 neutrons** for each cycle and **120 cycles (20 inactive and 100 active)** in a 3D core with fuel set at 950K and moderator set at 583K with **density 0.70 $\frac{g}{cm^3}$** .

2 | Reactivity Analysis

Table 2.1: NUWARD - Core Data

Core Height (m)	2,2
Pellet diameter (cm)	0,784
Pellet radius (cm)	0,392
Gap thickness (cm)	0,00832
Gap radius (cm)	0,40032
Clad thickness (cm)	0,0573
Clad radius (cm)	0,45762
Rod diameter (cm)	0,916
Axial power distribution	Chopped cosine
Axial power peaking factor	1,45
Pin Pitch (cm)	1,26

2.1. Moderator to fuel ratio

A preliminary topic of interest for the working group was **the characterisation of the k_{eff} curve** for different moderator to fuel ratios. The aim of this brief investigation was the characterisation of the working point of our reactor with regards to **under-moderated** or **over-moderated** conditions. Historically, **Pressurised Water Reactors** (PWRs) design was heavily influenced by the prevention of a **Loss of Coolant Accident (LOCA)**. Therefore the most diffused design choice for PWR reactors **was to ensure a slightly under-moderated condition** for the reactor at the beginning of its life; in this way, in case of a LOCA transient, the reactivity would decrease bringing about a **negative feedback** to this specific accident condition. Different accident scenarios involving the secondary circuit of the reactor (*eg.* Steam Line Break) would instead cause over-moderation and positive feedback during the transient, hence the chosen configuration should be as close as possible to the k_{eff} peak.

In order to evaluate the use of standardised PWR assemblies in an average-sized integral-PWR reactor, the group studied the variation of the multiplication factor as an effect of the change in rods' pitch. The k_{eff} -pitch curve for the reference core **reactor 0** (2.1) was graphed and the working point highlighted, confirming the under-moderated design.

Reactor Design	Number of Gd Rods	Gd %	U235 enrichment
Reactor 0	20	8%	5%

Table 2.2: Reactor 0 - Data

Pitch (cm)	k_{eff}
1	0,99
1,1	1,076
1,2	1,137
1,26	1,165
1,3	1,181
1,4	1,21
1,46	1,2
1,5	1,15

Table 2.3: k_{eff} -pitch results for Reactor 0

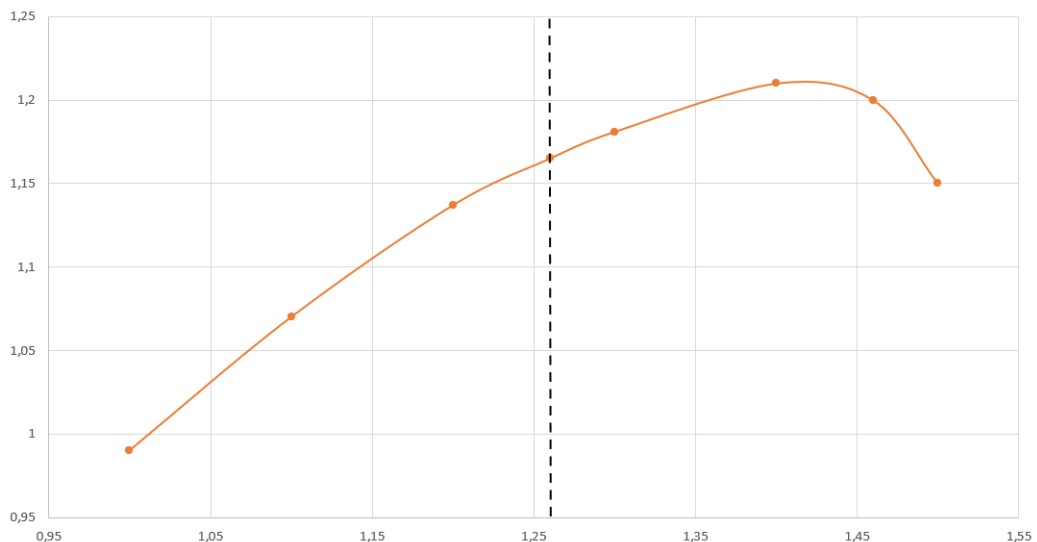


Figure 2.1: Reactor 0 | 20 Gd rods homogeneous distribution

2.2. Optimal enrichment and gadolinium

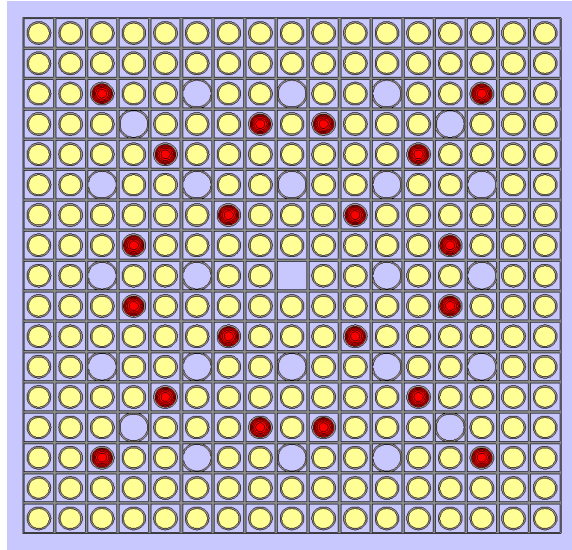


Figure 2.2: Reactor 0 | 20 Gd rods homogeneous distribution

In order to assess the modelling of our reactor's assemblies, we took into account several possible paths. As a starting point **the reference core reactor 0** (2.2) was analysed.

Bearing in mind the industrial, economical and geopolitical implications of enriching uranium beyond 5 % moving from **low enriched uranium (LEU)** to **high-assay low enriched uranium (HALEU)**, we positioned ourselves on the verge of the LEU area. Nonetheless, considering the economical opportunities of exploiting existing factories for the making of **standardised PWR assemblies**, we adopted a pitch of 1.26 cm.

The work group decided to investigate the role of **gadolinium enrichment** and **number of poisoned rods** on the reactor reactivity for this configuration. Such an approach was also meant to verify the accuracy of our model by comparing it with the results of the FLEXBLUE reactivity analysis [5]. The following results were gathered with this first attempt assembly design.

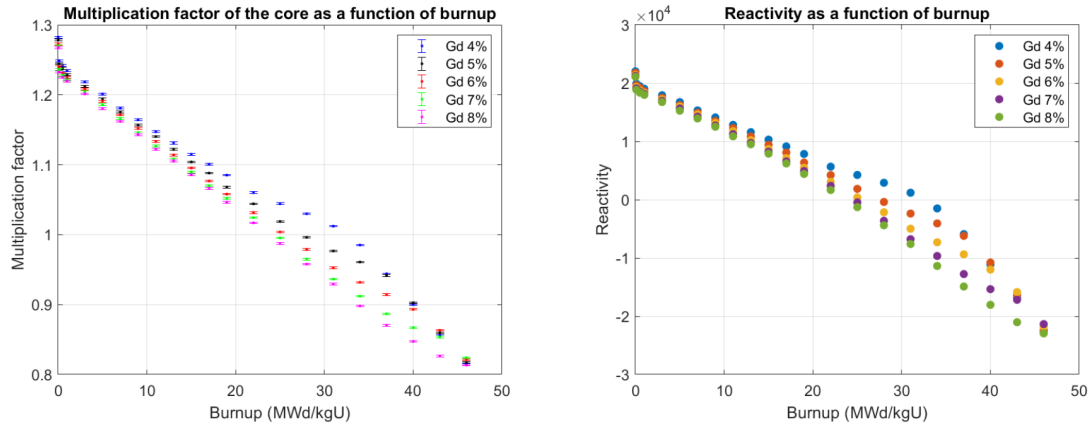


Figure 2.3: Reactor 0 | Reactivity and % Gd

Lowering gadolinium percentage brings about two intuitive effects:

- initial reactivity bumps up as a results of a lower macroscopic cross-section of absorption inside the core;
- a small gadolinium peak is reached at lower burn-ups as a result of quicker burning of poisoned fuel;

Despite the competitiveness of the Gd 4% configuration in terms of burnup, initial reactivity risks to position well beyond control rods worth. This suggests to drift towards other design solutions such as **the increase of the number of poisoned rods**.

The different configurations were tested both in the **infinite lattice** conditions and in the complete **3D core**, showing some riveting consequences.

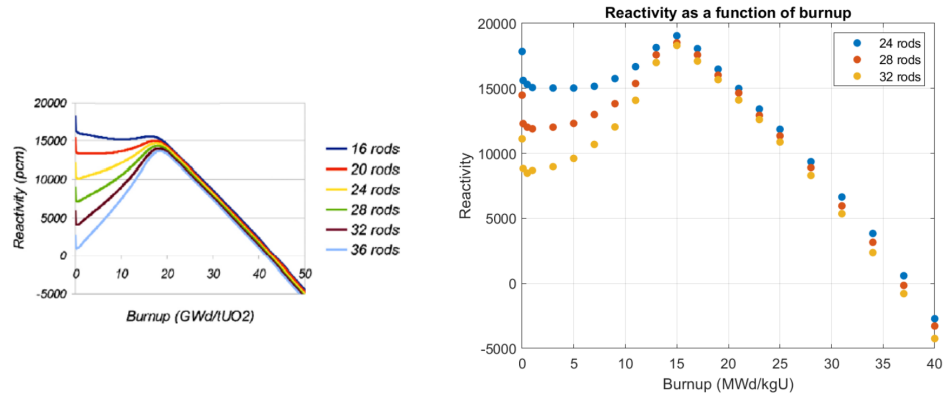


Figure 2.4: FLEXBLUE reference | Number of rods effect on 2D assembly

2D simulations show perfect consistency with the FLEXBLUE Reactivity Analysis [5]. In an infinite assembly the burning of gadolinium, being the Gd ratio the same in all rods, **is carried out with the same speed** showing no dependence on the number of rods. The latter only influence the initial reactivity, while **no significant change is brought about in the cut-off burnup**.

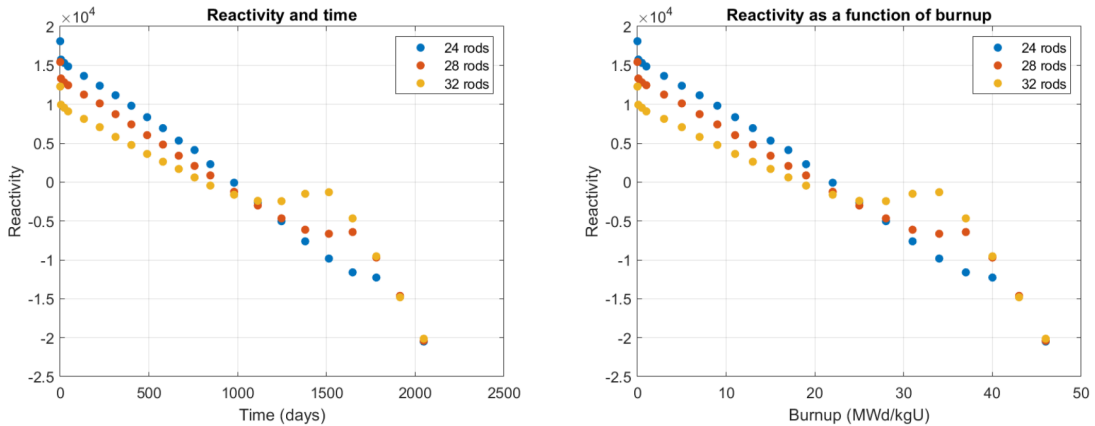


Figure 2.5: Number of rods effect on 3D assembly

On the contrary, 3D geometry shows an inversion in the reactivity happening at around 25 $\frac{MWd}{kgU}$. As a matter of fact, gadolinium content is consumed **more efficiently** when the **number of poisoned rods is higher**. This significant piece of information was further investigated by the working group using neutron flux and capture rate detectors in standard fuel and in the gadolinium rods, both in 2D and 3D geometry.

The calculation of the **neutron flux** in the 2D and 3D configurations, which results are summed up in appendix A, leads to some interesting observations that make justifiable the incongruities outlined above.

What can be seen at first is that in the 3D configurations the neutron fluxes are higher with respect to the 2D cases, actually in the 2D cases there is no **neutron leakage**, because of the reflective boundary conditions.

In all cases the neutron fluxes increase with time, in order to **guarantee the same power** despite the depletion of the fuel, and it is interesting to see that in the first part of fuel's life, when Gd has a high influence, **a higher flux is required to compensate its poisonous effect**, then when the effect of poisoned rods becomes negligible a **proportional increase** of the flux with the burnup is **restored**.

Since the power is fixed at 540 MW, also the reaction rate of fission has to be constant, this means that the more the Gd content and the more the neutron flux, so adding up the effects of increased neutron flux and increased number of poisoned rods there are different possible outcomes:

- in the 2D cores, as predictable, **the increase of neutron flux is proportional to the number of rods**, this means that in all the 2D configurations the Gd is consumed at the same speed, this can be seen also in the reaction rate over Gd;
- in the 3D configurations, since there is leakage, the increase of flux **is more than proportional** to the number of poisoned rods, this leads to a faster consumption of Gd. It means that the more the poisoned rods, the faster is the consumption of burnable absorber, as it can be seen in last column graphs concerning the Gd capture rate.

The previous considerations anticipate **the difficulties of reactivity control** and burnable poison content in **boron-free designs**, making the case for a drift towards higher uranium enrichment, moving from LEU to HALEU. Following simulations suggested to adopt a 7% – *wt* of uranium content and 5% – *wt* of gadolinium so to find a **compromise** between initial **reactivity sparks** and **cut-off burnups**. Nonetheless, the group decided to analyse the effects of differential poisoned rods positioning on the core lifetime and reactivity curve. Several geometries were taken into account, the most significant ones are analysed in the following section.

2.3. Selection of the best assembly geometry

Reactor Design	Gd Rods	Position	Gd %	U235 enrichment
Reactor 0	20	Homogeneous	5%	7%
Reactor 1	32	Homogeneous	5%	7%
Reactor 2	32	Cluster	5%	7%
Reactor 3	40	Mixed	5%	7%
Reactor 4	44	Mixed	5%	7%
Reactor 5	36	Mixed	5%	7%

Table 2.4: Core configurations

Results for **reactivity** and **burnup** calculations are reported here and commented in the table below:

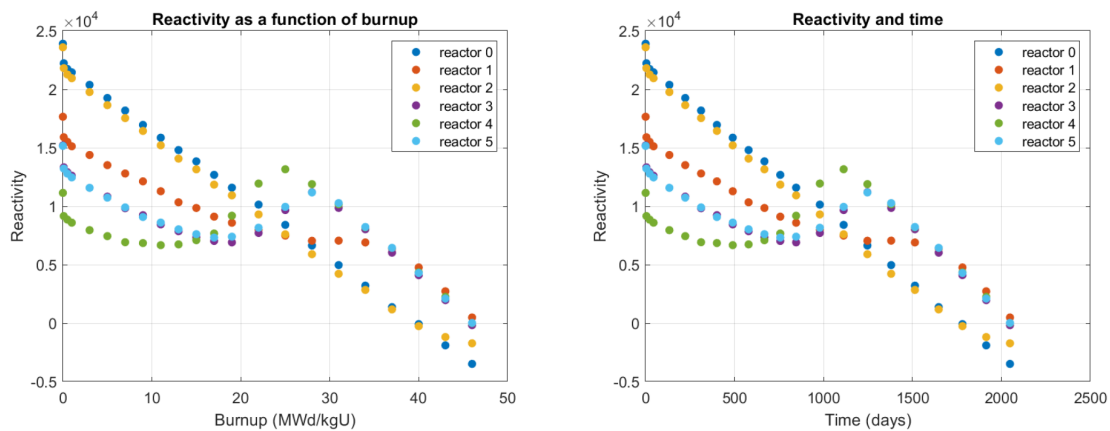


Figure 2.6: Reactivity results for different cores

The evaluated geometries involve changes in the position of the poisoned rods, going from a **totally homogeneous** distribution to totally clustered one, causing consequences to two parameters:

- **Initial reactivity**, since the initial reactivity depends on the effective surface of poisoned rods seen by the neutron flux, this parameter is strongly influenced by how much clustered are the Gadolinium rods;
- **Peak position**, the position of the peak is related to the consumption of Gd, which in turn is a function of the effective surface of the poisoned rods;

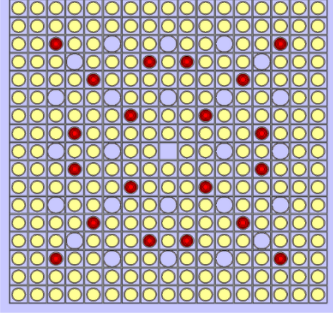
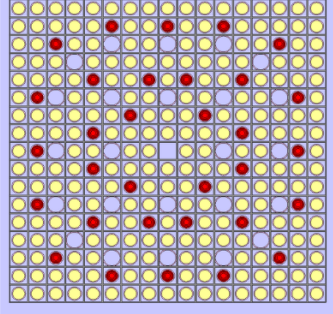
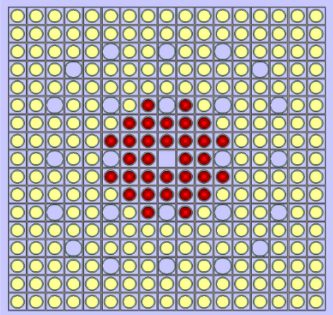
These two observations lead to the conclusion that a homogeneous core has **lower initial reactivity** and peaks at a **lower burnup**, meaning also that this peak is higher. Both these effects are due to gadolinium large effective surface in homogeneous cores. On the contrary, a **clustered core** has a **higher initial reactivity**, because of the reduced effective surface caused by a self-shielding effect of the Gd rods, but **the peak is moved towards higher burnups**.

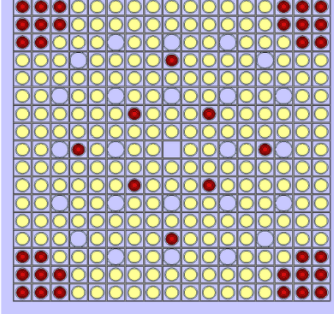
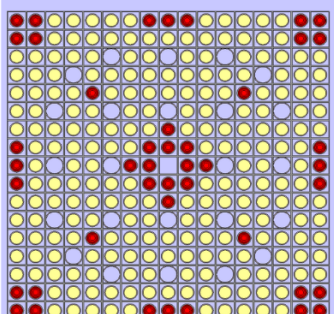
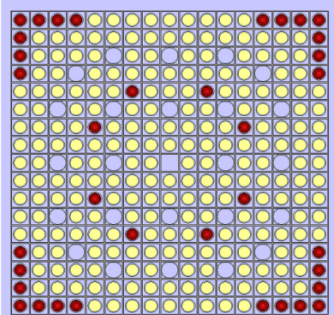
A mixed configuration seems to go somewhere optimising **the pros and cons of homogeneous and clustered geometries**. In this configuration, the assembly contains clusters of poisoned rods and isolated poisoned rods homogeneously distributed among the clusters. In this configuration **reactivity** at the beginning of life can be set by the number of **isolated poisoned rods** and the **peak reactivity** can be controlled by acting on the **size of the cluster**. Moreover, considering that an assembly is not alone in the core, it should be kept in mind that the clusters on the edge are adjacent to the clusters of other assemblies, making overall bigger clusters.

In the following geometry discussion, the effects of the number of rods and their position combines with the **alteration of the neutron flux** brought about by a greater number of poisoned rods.

The Reactor 4's assembly geometry was not the only one that showed precise and agreeable characteristics: also reactor 3 and 5 presented good and interesting results, but their curves started, practically overlapped, at higher reactivity values. This **higher reactivity contribution** seems to be unreasonable for a safe control of the reactor during the beginning of life (BOL), hence our choice fell on **Reactor 4**.

The overall results are discussed below.

Assembly design	Main results
 Reactor 0	<p>This is the reference configuration with 20 homogeneously distributed poisoned rods. The overall reactivity is reduced, but the low number of rods does not affect very much the initial reactivity, which is definitely high at 24 000 pcm. Moreover, due to slow Gd consumption, the peak cannot be seen during fuel's life that ends at 40MWd/kgU. An alternative homogeneous configuration has been tested in order to improve the homogeneous design.</p>
 Reactor 1	<p>32 homogeneously distributed poisoned rods. Compared to Reactor 0, the influence of Gd is stronger and it actually lowers the reactivity to 17 000 pcm. There is a tiny peak, due to a faster consumption of Gd, at 32MWd/kgU. The life of fuel is extended to 47MWd/kgU.</p>
 Reactor 2	<p>This is the totally clustered geometry with a cluster of 32 rods at the center of the assembly. Even if the number of rods is the same of reactor 1, being the effective surface very low, the initial reactivity is 24 000 pcm. Self shielding of gadolinium limits its initial consumption, causing extra anti-reactivity later on in the life of the reactor.</p>

Assembly design	Main results
 Reactor 3	<p>This is a mixed configuration with 40 rods divided in 4 clusters and 8 rods homogeneously distributed. The initial reactivity of 15 000 pcm is much lower than the other cases because of a good trade-off between clusterization and homogeneous rods. The Gd effect runs out at 28MWd/kgU guaranteeing a satisfying cut-off burnup of 46MWd/kgU.</p>
 Reactor 4	<p>This mixed configuration, with 44 rods, makes this reactor the one with the highest neutron flux. A very wise clusterization guarantees a large effective surface, that allows an easy-to-control initial reactivity of 11 000 pcm, then, due to the great consumption of Gd, there is a peak at 25MWd/kgU and the fuel ends its life with a good burnup at 46MWd/kgU.</p>
 Reactor 5	<p>This is a mixed configuration with 36 rods, where 8 are distributed homogeneously and the other 28 are arranged as a frame, this increases the effective surface allowing an initial reactivity of 15 000 pcm, and then the evolution is basically the same of reactor 3.</p>

3 | Characterisation of fuel performance coefficients

3.1. Temperature Coefficients

In order to evaluate the stability of the selected core design, it is essential to study **the changes in reactivity** brought about by **temperature variations**, this is made by means of the **temperature coefficients** defined by the relation:

$$\alpha_T = \frac{\partial \rho}{\partial T} \quad (3.1)$$

and being $\rho = \frac{k_{eff}-1}{k_{eff}}$

$$\alpha_T = \frac{1}{k_{eff}^2} \frac{\partial k_{eff}}{\partial T} \quad (3.2)$$

Where ρ is the reactivity and T can be the temperature of the fuel T_F or the temperature of the moderator T_M . To operate a stable core, since α_T has the same algebraic sign of $\frac{\partial k_{eff}}{\partial T}$, it is necessary to have always negative α_T , because if α_T is positive after an insertion of positive reactivity (*e.g.* sudden removal of control rod) the reactor would be subject to an increase of temperature, causing a further increase of reactivity and leading to the need of external intervention. On the contrary a negative α_T is a stabilizer that takes back the reactor to its operating point if there are tiny changes in reactivity. Nonetheless, a large absolute value of α_T causes a tiny increase of temperature that may result in a large drop in reactivity that makes the reactor subcritical [8]. Being α_T itself a function of temperature it is important to calculate the values in a large range of operating temperatures in order to verify negative feedback in all working conditions.

3.1.1. Fuel Temperature Coefficient

The **fuel temperature coefficient**, also called prompt temperature coefficient because the fuel's temperature is the first to change consequently to a change in power, is defined as follows:

$$\alpha_F = \frac{\partial \rho}{\partial T_F} \quad (3.3)$$

This coefficient has been calculated for NUWARD reactor by evaluating reactivity after changing the temperature of the fuel in the 300K-1500K range with a 300K step and keeping constant all the other parameters.

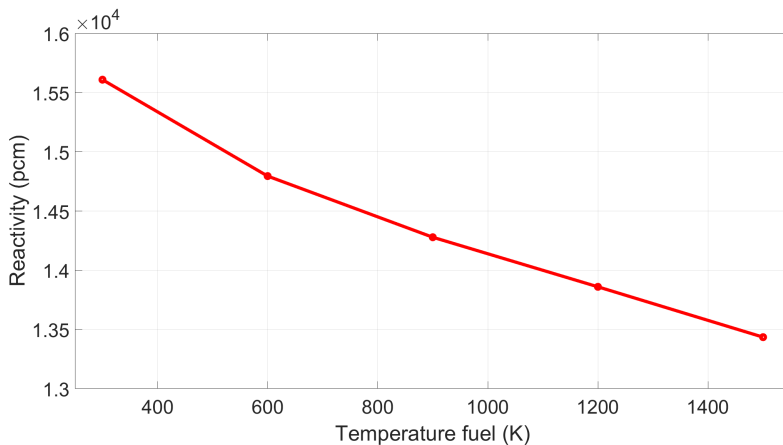


Figure 3.1: Reactivity as a function of the temperature of the fuel

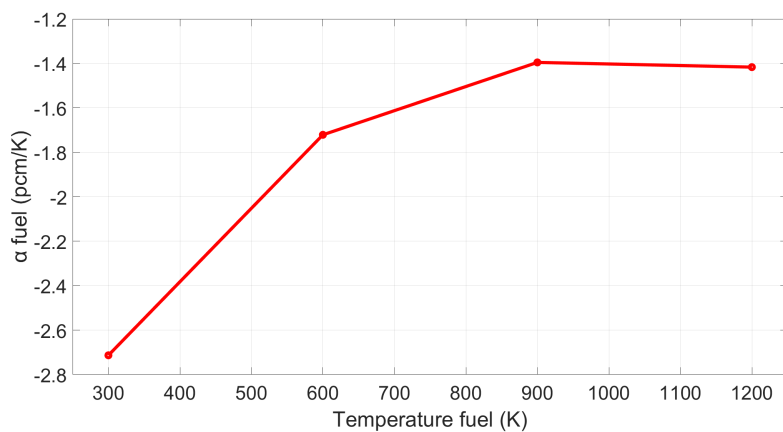


Figure 3.2: Fuel Temperature Coefficient as a function of the temperature of the fuel

The results show, with a confidence interval of $\pm 0.16\%$ on the K_{eff} , that α_F stays between $-2.7 \frac{pcm}{K}$ and $-1.4 \frac{pcm}{K}$ with an average value of $-1.8 \frac{pcm}{K}$, since the typical values for a PWR cited in literature are between $-4 \frac{pcm}{K}$ and $-1 \frac{pcm}{K}$ [9], this can be considered a satisfactory result.

The reason behind this negative α_F has to be traced back to the **doppler-broadening of fuel resonances** that are increased with temperature, reducing reactivity. Being α_F sensitively dependant on fuel composition, since the calculations are made on the fresh core, the fertile U^{238} covers a leading role in resonant absorption, making the obtained value of α_F quite clear to understand.

Another important issue that guarantees the negativity of α_F is the very same presence of Gd_2O_3 , actually Gd has resonant absorption like U^{238} so its effect is added to the one of U^{238} [10].

3.1.2. Moderator Temperature Coefficient

The moderator temperature coefficient, that in the case of a LWR is equal to the coolant temperature coefficient, is defined as follows:

$$\alpha_M = \frac{\partial \rho}{\partial T_M} \quad (3.4)$$

This coefficient has been calculated by evaluating reactivity after changing the temperature of the moderator in **the 300K-600K range with a 100K step**, and consequently changing the density (calculated as the density of water at T_M and 155 bar), and keeping constant all the other parameters.

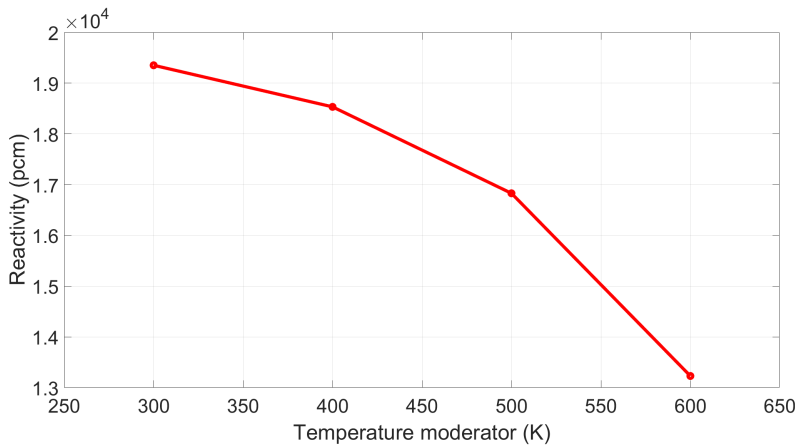


Figure 3.3: Reactivity as a function of the temperature of the moderator

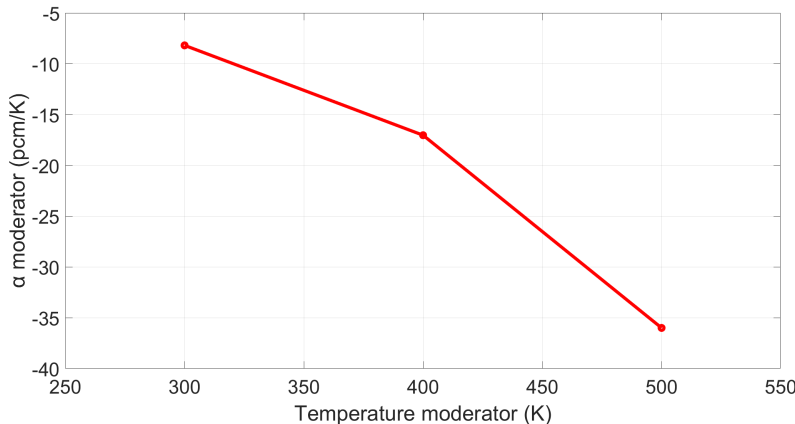


Figure 3.4: Moderator Temperature Coefficient as a function of the temperature of the moderator

The results show, with a confidence interval of $\pm 0.04\%$ on the K_{eff} , that α_M stays between $-36 \frac{pcm}{K}$ and $-8 \frac{pcm}{K}$ with an average value of $-20.5 \frac{pcm}{K}$, since the typical values for a PWR are between $-50 \frac{pcm}{K}$ and $-8 \frac{pcm}{K}$ [9], this can be considered a satisfactory result.

This result can be linked to two intuitive causes, in order of significance. The first is that an increase of moderator temperature brings about **a decrease of density** that turns out in a loss of moderation; being the reactor under moderated this will cause lower reactivity. The second reason is that an increased temperature of the moderator **hardens the neutron spectrum**, thus increasing resonant absorption in the fuel[11].

Another important factor that influences α_M in this core is the absence of boron that would have usually maintained a largely negative moderator temperature coefficient [12].

3.2. Power Coefficient

Flexibility in the operation of a nuclear reactor and enhanced **load following** characteristics are widely regarded as important features for effective integration of small modular reactors in hybrid energy systems. Bearing this in mind, characterisation of the reactor behaviour by means of a unified coefficient depending on a fairly easy to measure quantity may represent a useful indicator.

Practical application of feedback coefficients such as the above-defined ones are made difficult by the fact that **the fuel temperature is not directly controlled by standard measuring channels**. Therefore describing the effects of **reactor power change** on reactivity may appear extremely convenient.

There is few agreement on a unified definition for this parameter. We will limit ourselves to the most commonly used one: power coefficient represents the change in reactivity caused by the single power variation [13], with the specification of:

- determining the new power level only after stabilisation;
- keeping the temperature at the core inlet constant;

Power coefficient can be therefore interpreted as an aggregate of both **fuel and moderator coefficient**, considering partial derivatives as follows:

$$\alpha_P = \frac{\partial \rho}{\partial P} \quad (3.5)$$

$$\alpha_P = \alpha_F \frac{dT_F}{dP} + \alpha_M \frac{dT_M}{dP} \quad (3.6)$$

In the context of a SERPENT simulation, a quick change in the *set power* parameter would be insufficient to determining a new working point, since the power is here used only for neutron flux normalisation. Hence, an acceptable estimate of the new conditions of fuel and moderator for different power levels had to be determined. The *materials input source* was then updated with the newly defined conditions and the proper thermal libraries for water.

Fuel and coolant temperature were estimated using a simplified heat transfer relation and imposing a linear evolution of coolant average temperature with power.

$$Q = K(T_F - T_M) \quad (3.7)$$

where K is an approximated global heat transfer coefficient, T_F is the temperature of the fuel, T_M is the temperature of the coolant. The following working points were simulated.

Power Level	Fuel Temp (K)	Mod Temp (K)	Mod Density (g/cm3)
540 MW (100 %)	950	583	0,70602
378 MW (70 %)	828,9	572	0,7285658
216 MW (40 %)	709,8	563	0,7462010
54 MW (10 %)	590,7	554	0,7625381

Table 3.1: Power coefficient - Input parameters

Results for static criticality source simulation are summarised in 3.5

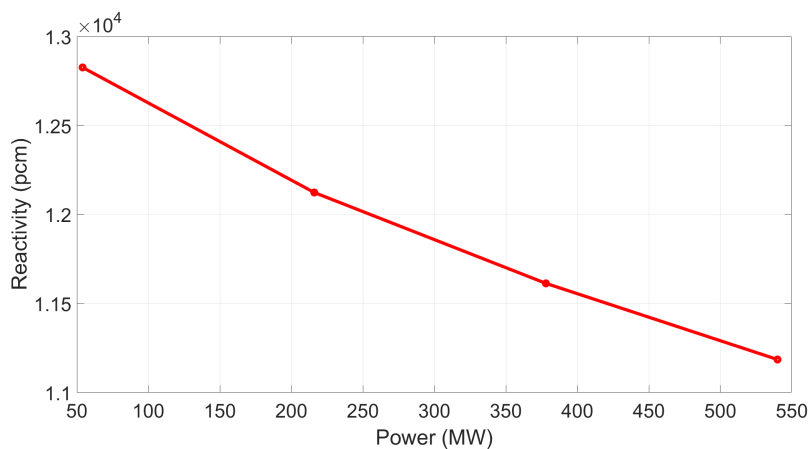


Figure 3.5: Reactivity as a function of power

Considering the maximum and minimum values in the power interval, the power coefficient settles at around $-3.3 \frac{pcm}{MW}$ as a mid value, with a confidence interval on the k_{eff}

of $\pm 0.12\%$. Nonetheless, it does not change consistently in the considered power range, which is another useful characteristic for a practical and easy to use indicator [13].

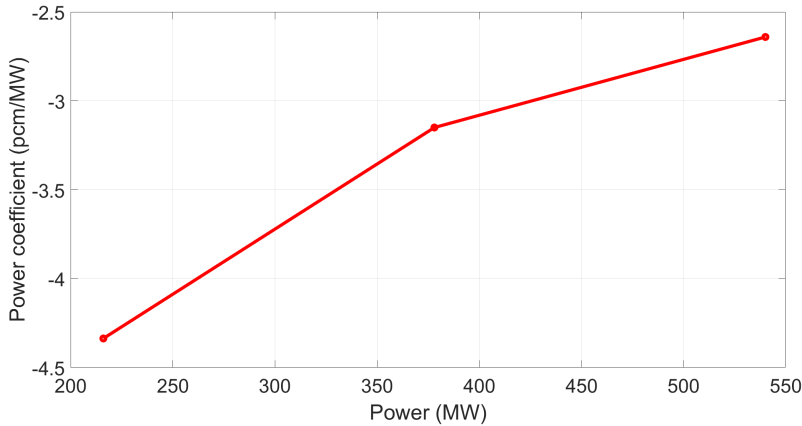


Figure 3.6: Power coefficient as a function of power

3.3. Void Coefficient

The void coefficient is defined as the change in reactivity due to the change in void fraction, where the void fraction x is **the fraction of the total volume occupied by void**:

$$\alpha_V = \frac{\partial \rho}{\partial x} \quad (3.8)$$

This coefficient is closely related to the Moderator Temperature Coefficient, since void is a particular condition in which water has very low density, so involving the above-mentioned effects of this issue. This means that, to operate a stable core, it is necessary a negative α_V .

The calculations have been carried out implementing a *void assembly* in which water is at the density of saturated vapor at 155 bar, then this assembly has been substituted in an increasing number of positions in order to assess reactivity for different void fractions in the reactor. The different arrangements that have been tried involve the substitution of 1, 3, 6, 8, 10 normal assemblies with *void assemblies* with the following results

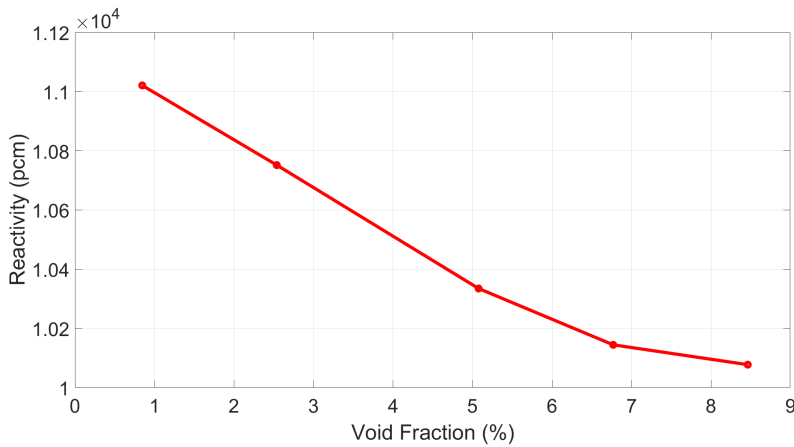


Figure 3.7: Reactivity as a function the of void fraction x

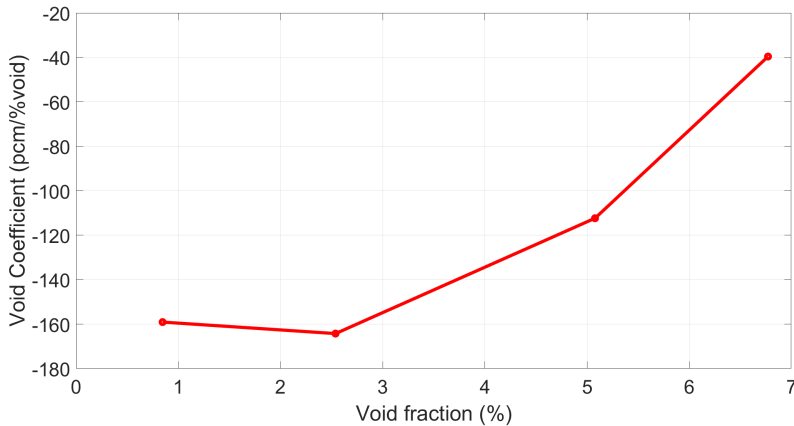


Figure 3.8: Void Coefficient as a function of the void fraction x

The results show, with a confidence interval of $\pm 0.15\%$ on the k_{eff} , that α_V is between $-163 \frac{\text{pcm}}{\% \text{void}}$ and $-40 \frac{\text{pcm}}{\% \text{void}}$ with an average value of $-124 \frac{\text{pcm}}{\% \text{void}}$, so this result is consistent with the necessity of a negative feedback.

This coefficient is **more negative than the Moderator Temperature** one because void has a harder impact on reactivity, furthermore since this is a boron free reactor the moderating effect of water is predominant over absorption, so this coefficient is largely negative.

Differently from other coefficients, it is very important to assess **the position** in which void is located. Intuitively, the altered assembly has a higher impact if there is a higher neutron flux, thus an analysis of the reactivity has been made using a single *void assembly* but in different positions.

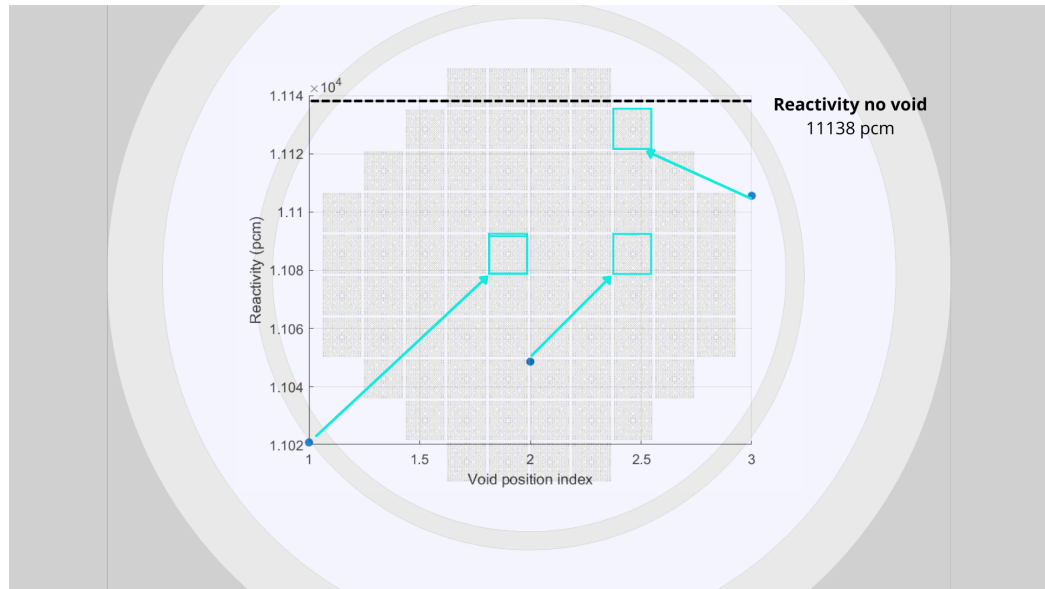


Figure 3.9: Reactivity as a function of void position

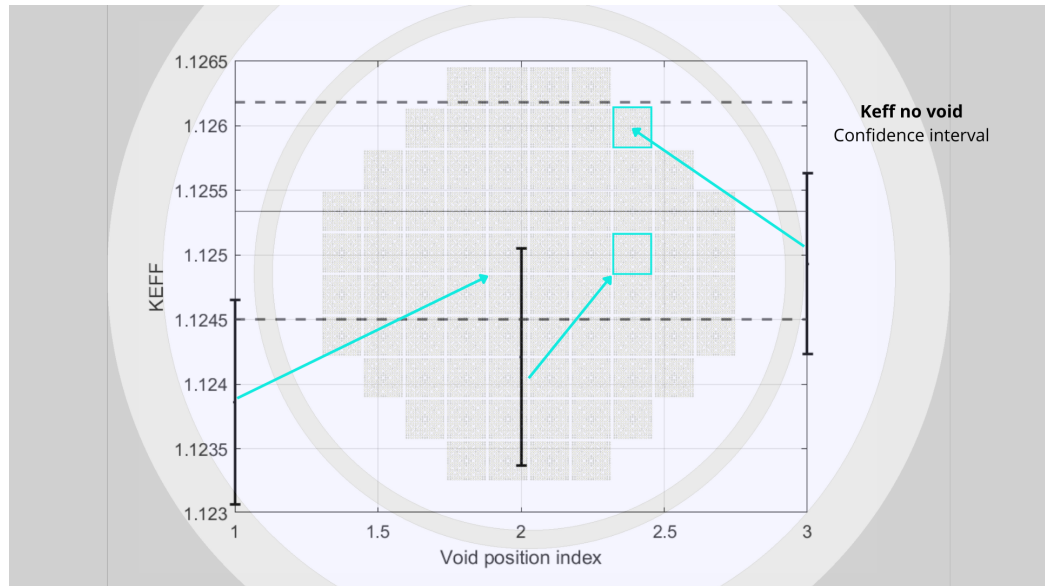


Figure 3.10: Keff as a function of void position

As expected, **negative reactivity feedback** is more evident when **void is located near the centre of the core**.

4 | Reactivity Control

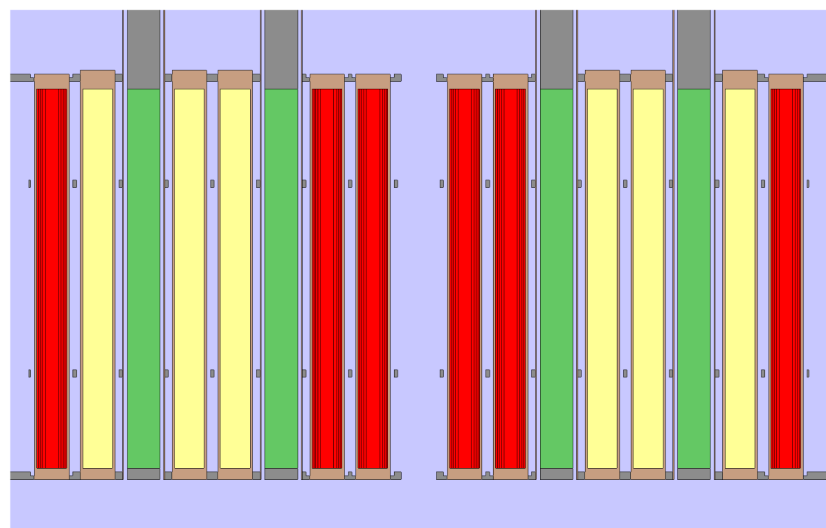


Figure 4.1: Control rods inserted in assembly type reactor 4 | section view

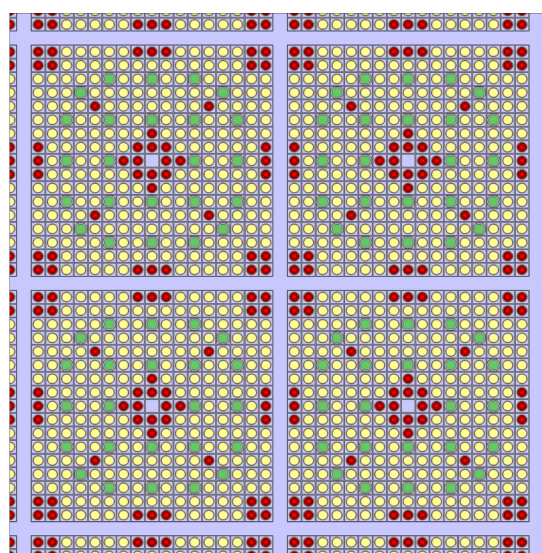


Figure 4.2: Control rods inserted in assembly type reactor 4 | upper view

Reactivity control in integral PWRs is often made difficult by the design choice to **avoid soluble boron** as a reactivity control mechanism. The burden of keeping the reactor critical is therefore only on the control rods, which normally serve a two-pronged function [8]:

- they are inserted rather **quickly** during **startup**, shutdown and changes in power;
- they are moved **slowly** to compensate for fuel burnup and other long-term changes in the reactor core;

The effect of the control rod in the two cases is significantly different. While in case of a slow insertion the reactor is likely to remain critical or nearly so, a quick insertion can lead to a subcritical or supercritical response. The definition of **control rod worth** varies in the two cases. For the sake of this research and conscious of the limits of static criticality simulations (no transients), we will consider the following definition for control rod worth and we will refer it to the totality of the boron carbide rods inserted:

$$\rho_w = \frac{1 - k}{k} \quad (4.1)$$

Where k is the multiplication factor after control rods insertion.

Simulations for reactivity control were meant to evaluate the control rods' ability to ensure a proper **anti-reactivity margin** if inserted in the core. **Cold shutdown conditions** were considered in the materials input source, recreating one of the most stressing scenarios for the reactor: cold fuel, cold moderator and low power. The following inputs were considered:

Material	Temperature	Pressure
Moderator	93 °C	1 bar
Fuel	97 °C	
Cladding	100 °C	

Table 4.1: Cold Shutdown conditions

Multiplication factor with CRs fully withdrawn amounted at 1.14713, while with control rods fully inserted k_{eff} collapsed at 0.77738, with a confidence interval of $\pm 0.12\%$. Control rods were not clustered in control groups, but instead **they were moved jointly**

inside the core. Their worth proved to be sufficient to ensure reactivity control even without the help of soluble boron.

Nonetheless, control rods insertion brings about **the alteration of the power profile** along the fuel. We decided to assess this issue by computing a meaningful parameter for reactor core power transients: the **power axial offset**.

$$AO = \frac{POW_{UP} - POW_{DOWN}}{POW_{UP} + POW_{DOWN}} * 100 \quad (4.2)$$

Axial offset is defined as reported, where:

- POW_{UP} is the power in the upper half of the core
- POW_{DOWN} is the power in the lower half of the core

High values of power AO in load following transients may bring about **differential expansion, mechanical stresses and, eventually nucleate boiling**. Moreover, the **higher enriched fuel configuration we chose (HALEU)**, may bring about an increase in crud deposition which can naturally lead to **greater axial power offset**. Since power plants have limits on this kind of phenomenon, it must be studied carefully. [14]

The definition of the problem now focused on the identification of the position of the control rods so to insert the anti-reactivity necessary for moving from 100 % power to 10 %. Not having the possibility to dynamically simulate the control rods movement and their effect on the input parameters (power, temperature of the moderator, temperature of the fuel etc.), the construction of a proper CR calibration curve seemed to be an ill-fated task. Therefore, we decided to take the conditions of the core at 10% power as an input and to compute the reactivity for different CR positions. Hence, an approximated calibration curve was built and the chosen CR depth was so that anti-reactivity insertion equalled the reactivity boost from 100 % to 10 % as suggested by the power coefficient (3.5). **CR position was in the end chosen at 45%** in order to meet the above-mentioned requirements.

In order to compute axial power, a **fission rate detector** discretized with twenty bins on the z-axis was defined. No specific cluster of assemblies was considered, the detector computed reactions in the whole core so to have better statistics.

CR position	Keff	ρ (pcm)	CR worth (pcm)	Antireactivity insertion (pcm)
100%in	0,7773	-28637,217	28637,217	41462,217
80%in	1,02679	2610	-2610	10215
60%in	1,0994	9042	-9042	3783
40%in	1,12815	11360	-11360	1465
0%in	1,1471	12825	-12825	0

Table 4.2: Antireactivity inserition and CR position

Results for AO were in the range of safe values defined in recent SMR reactivity analysis carried out at Electricité de France (EdF)[15] .

Position (cm)	Power (full power, no rods, W)	Power (10% power, rods 45%, W)
-95	9.63E+06	2.48E+06
-85	1.45E+07	3.66E+06
-75	1.95E+07	4.73E+06
-65	2.40E+07	5.41E+06
-55	2.52E+07	5.53E+06
-45	2.98E+07	5.87E+06
-35	3.57E+07	6.30E+06
-25	3.87E+07	5.93E+06
-15	4.08E+07	5.17E+06
-5	4.09E+07	4.06E+06
5	4.05E+07	2.53E+06
15	3.90E+07	9.42E+05
25	3.66E+07	4.08E+05
35	3.33E+07	1.80E+05
45	2.72E+07	7.58E+04
55	2.26E+07	3.18E+04
65	2.03E+07	1.65E+04
75	1.63E+07	6.83E+03
85	1.18E+07	2.95E+03
95	7.03E+06	1.52E+03

Transient type	AO
Load following	-70,8

Table 4.3: Axial offset results

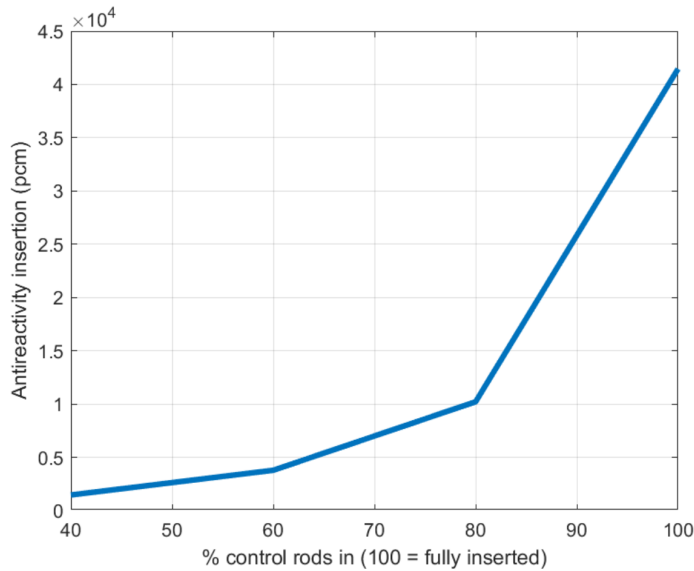


Figure 4.3: Approximated anti-reactivity insertion curve for CRs group

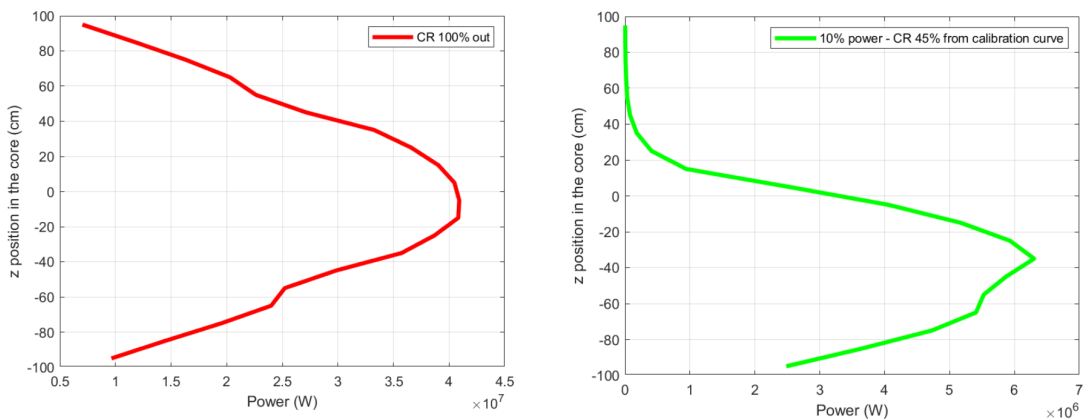


Figure 4.4: Power profile | control rods fully out | control rods 45 % in

5 | Future developments

In light of the results obtained with this projects, the working group would like to briefly introduce possible future developments to extend the research.

- Refuelling strategies
- MOX as NUWARD reactor fuel
- Thermal analysis of the fuel

REFUELLED STRATEGIES

The purpose of refuelling is to achieve a long cycle in order to maximise the availability of the reactor. With regards to NUWARD reactor it is possible to opt for a **half core or a full core refuelling strategy**. Different strategies bring about different consequences: **two-batch** cycle generates **unoptimized core power distribution**, which causes a reduction of maximum linear power, while the **single batch cycle** calls for a **better power distribution** optimization. In light of these differences, best core geometries for **two-batch cycle** is the **classic homogeneous configuration** of Gd poisoning, which can ensure quite good safety performances; for **the single batch cycle**, the best solution is to opt for **heterogeneous configurations** of Gd inside the fuel assembly.

The working group suggests assessing the economical implications on the Levelised Cost of Electricity (LCOE) of both strategies and core designs.

MOX

MOX fuel (mixed oxide fuel) is a nuclear fuel usually composed of not only Uranium oxide (natural, reprocessed, or depleted uranium) but also of **plutonium oxide**. MOX fuel is an alternative to the low-enriched uranium fuel (used in the light-water reactors), which is predominant in the nuclear power generation. Analysing MOX fuel could be very interesting because Plutonium-239 comes along with interesting physical

characteristics and important economical and geopolitical implications:

- **physics:** the average number of neutrons per fission is higher;
- **economics:** implementation of MOX fuel requires investment on reprocessing facilities;
- **geopolitics:** political and social concerns due to plutonium proliferation must be taken into consideration;

The working group would suggest repeating the reactivity analysis with plutonium enriched fuel, assessing the behaviour of gadolinium coupled with MOX. The assessment of refuelling strategies ought to be taken into consideration too.

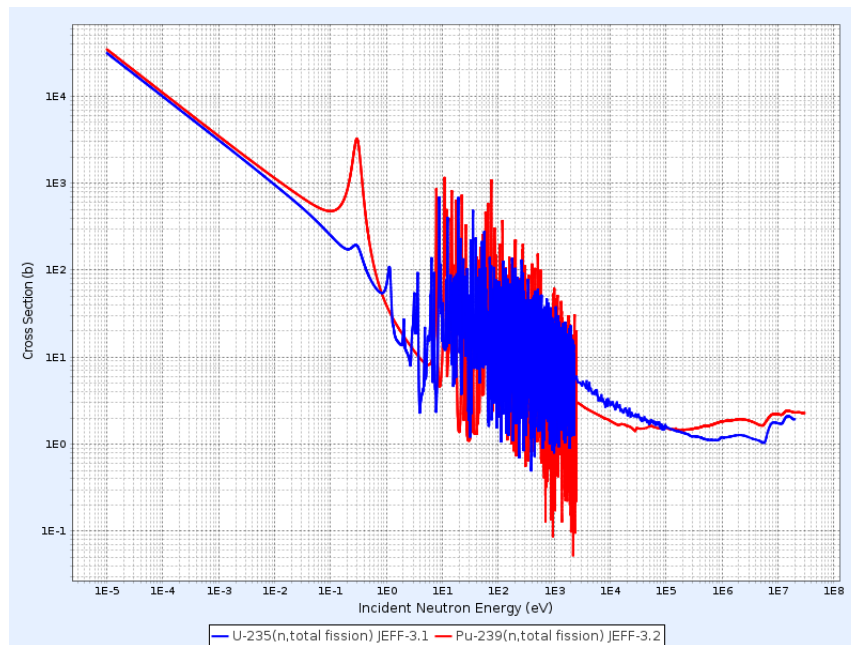


Figure 5.1: U-235 and Pu-239 fission cross sections | KAERI

THERMAL ANALYSIS

Using SERPENT code limits the reactivity analysis to neutronics and power data. The coupling of SERPENT code with the **FINIX fuel performance module** could extend the research to temperature evolution in the fuel in normal operation and accident conditions.

Bibliography

- [1] H. Kamide, G. Rodriguez, P. Guiberteau, N. Kawasaki, B. Hatala, A. Alemberti, S. Bourg, Y. Huang, F. Serre, M. A. Fuetterer, *et al.*, “Generation iv international forum-gif, annual report 2020,” 2021.
- [2] E. Commission, “Eu taxonomy draft,” vol. 1, pp. 9–10, 2021.
- [3] E. Hanus, “Nuward cea presentation,” 2019.
- [4] IAEA, “Nuward info sheet,” *ARIS database IAEA*, 2019.
- [5] J.-J. Ingremoine and M. Cordiez, “Flexblue® core design: optimisation of fuel poisoning for a soluble boron free core with full or half core refuelling,” *EPJ Nuclear Sciences & Technologies*, pp. 1–13, 2015.
- [6] CEA, “Direction de l’energie nucleaire | rapport d’activité,” 2019.
- [7] J. Leppänen *et al.*, “Development of a new monte carlo reactor physics code,” 2007.
- [8] J. R. LAMARSH, “Introduction to nuclear reactor theory,” pp. 448–450, 1966.
- [9] J. J. Duderstadt and L. J. Hamilton, “Nuclear reactor analysis,” p. 563, 1976.
- [10] A. Shahmirzaei, G. Ansarifar, and A. Koraniany, “Assessment of gadolinium concentration effects on the nuscale reactor parameters and optimizing the fuel composition via machine learning method,” *International Journal of Energy Research*, vol. 46, no. 7, 2022.
- [11] J. J. Duderstadt and L. J. Hamilton, “Nuclear reactor analysis,” p. 559:561, 1976.
- [12] J. J. Duderstadt and L. J. Hamilton, “Nuclear reactor analysis,” p. 554:556, 1976.
- [13] Y. Kazansky and Y. Slekenichs, “Power coefficient of reactivity: definition, interconnection with other coefficients of reactivity, evaluation of results of transients in power nuclear reactors,” *Nuclear Energy and Technology*, vol. 4, p. 111, 2018.
- [14] L. Carlson, J. Miller, and Z. Wu, “Implications of haleu fuel on the design of smrs and micro-reactors,” *Nuclear Engineering and Design*, vol. 389, p. 111648, 2022.

- [15] E. G. Niccolo Ludovico Coscia, “Amelioration des mod’eles de cin’etique spatiale pour les rep : application aux ‘etudes des transitoires incidentels et de fonctionnement des coeurs n4 et small modular reactor,” *EDF RD Département SINETICS*.

A | Appendix A

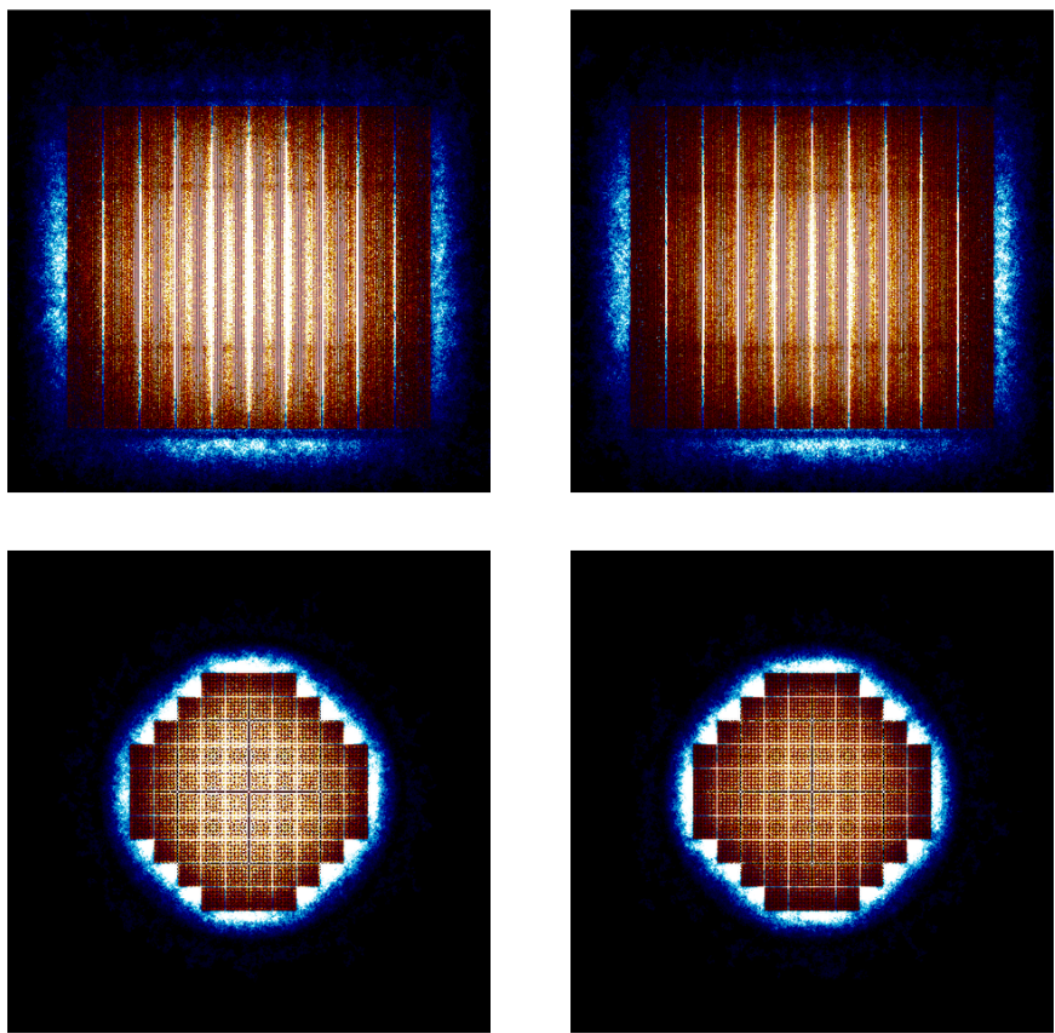
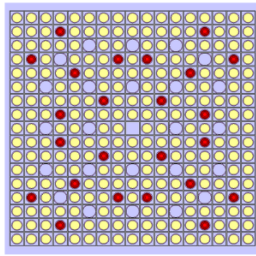


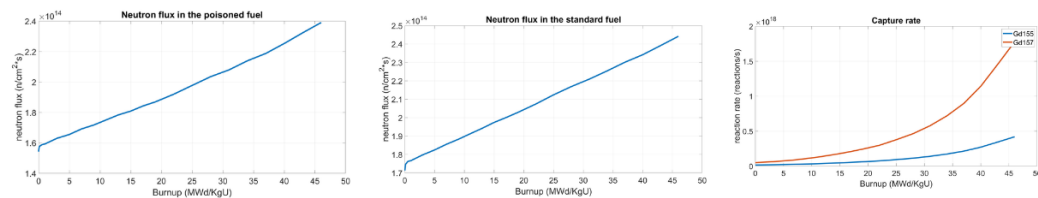
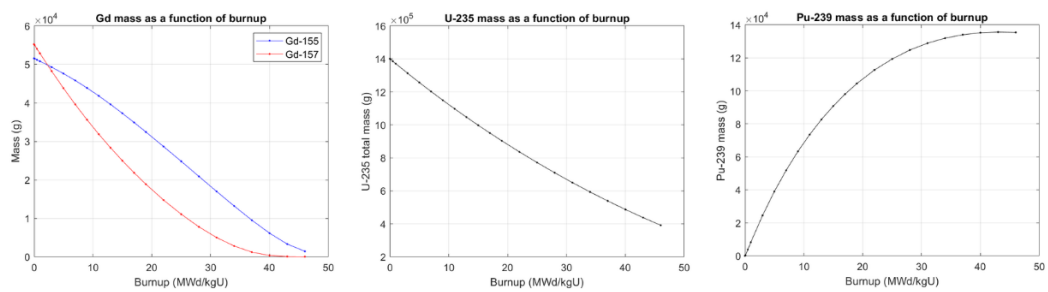
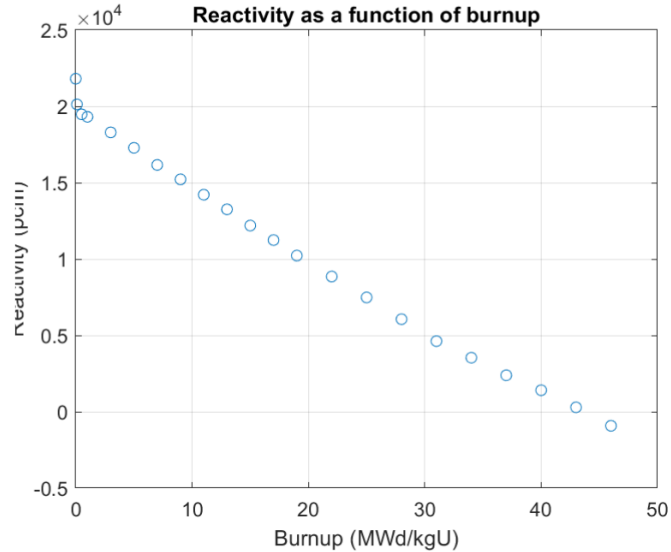
Figure A.1: Burnup mesh - section and axial view - BOL and EOL

Poisoned Rods

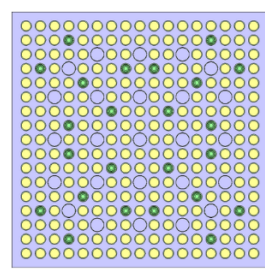
Neutron flux in the standard fuel, in poisoned rods and Gd capture rate



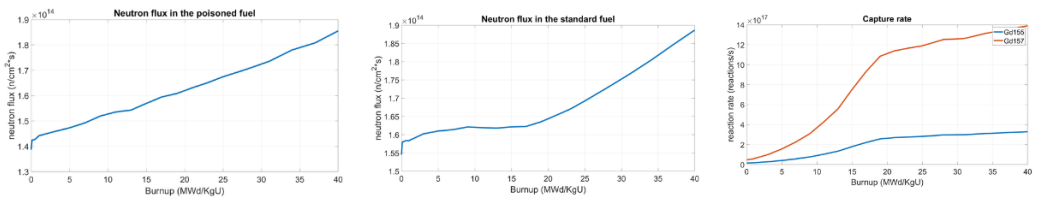
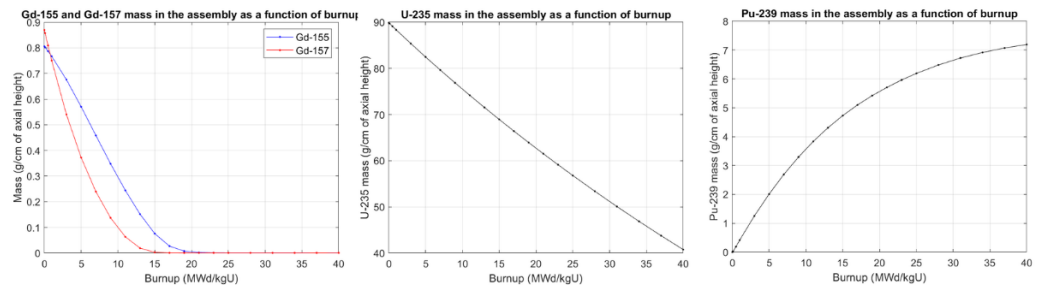
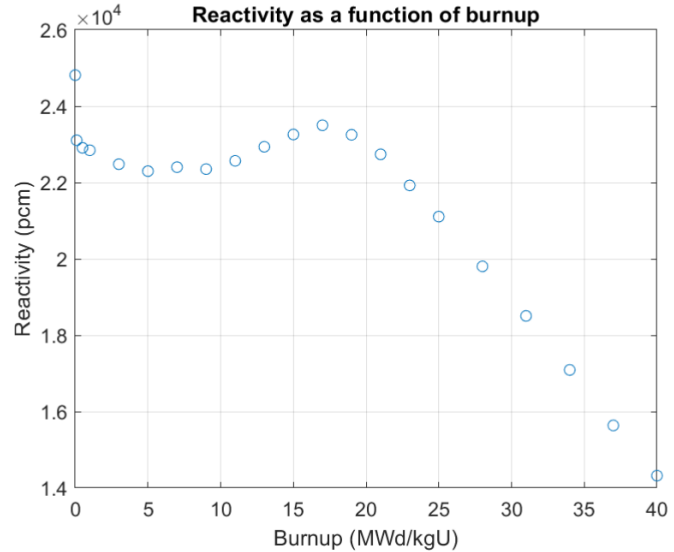
24 rods | 3D



Poisoned Rods Neutron flux in the standard fuel, in poisoned rods and Gd capture rate

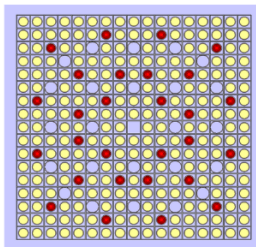


24 rods | 2D

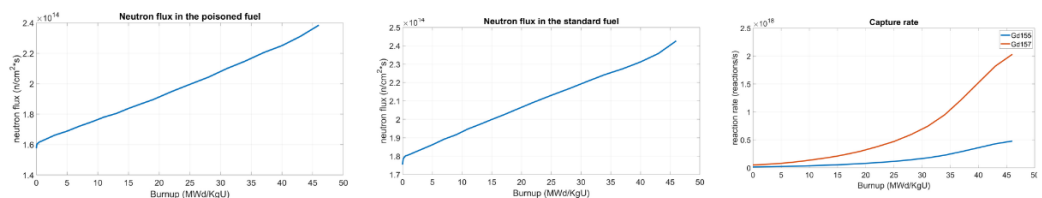
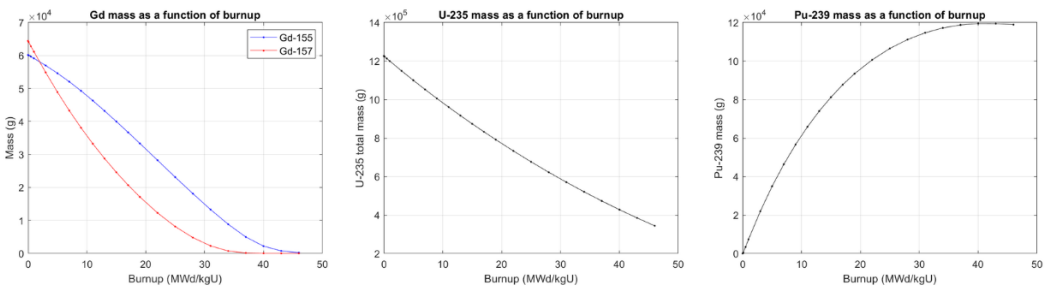
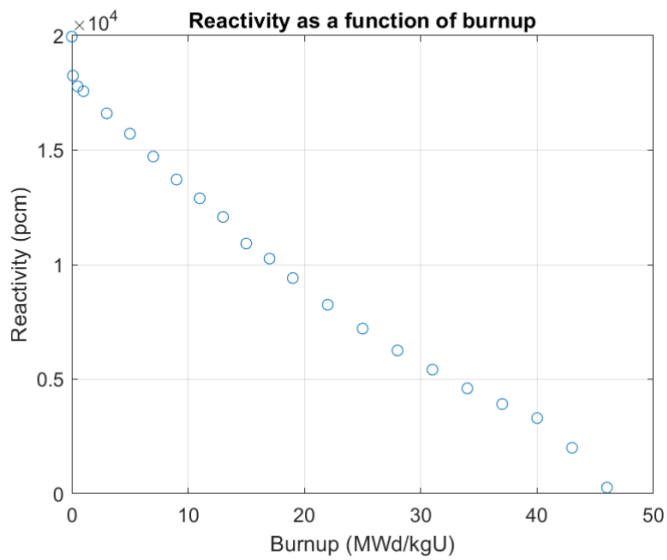


Poisoned Rods

Neutron flux in the standard fuel, in poisoned rods and Gd capture rate

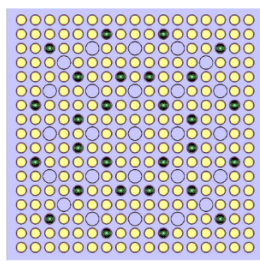


28 rods | 3D

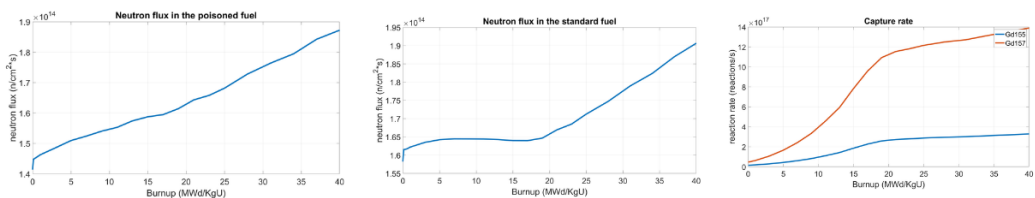
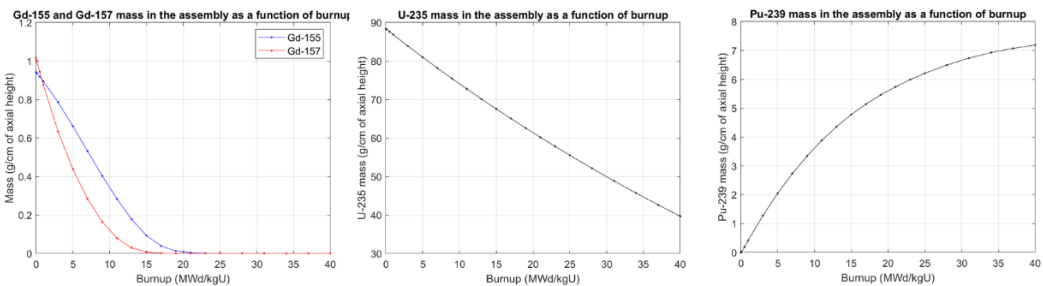
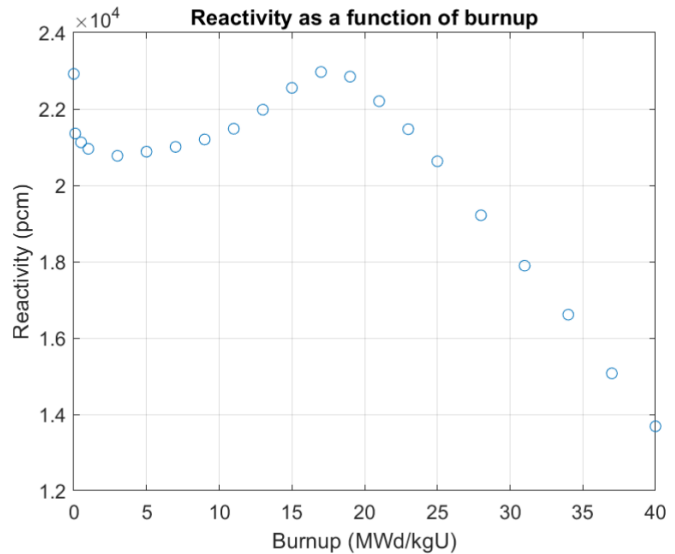


Poisoned Rods

Neutron flux in the standard fuel, in poisoned rods and Gd capture rate

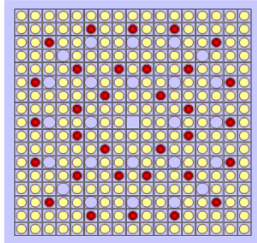


28 rods | 2D

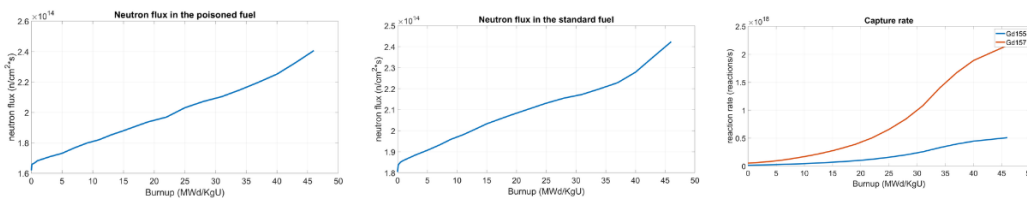
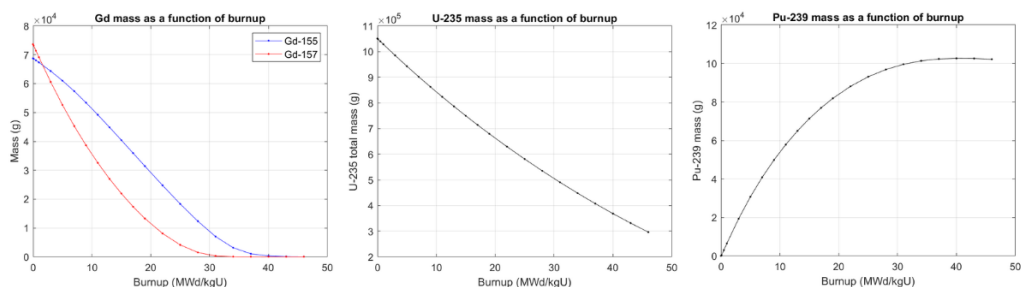
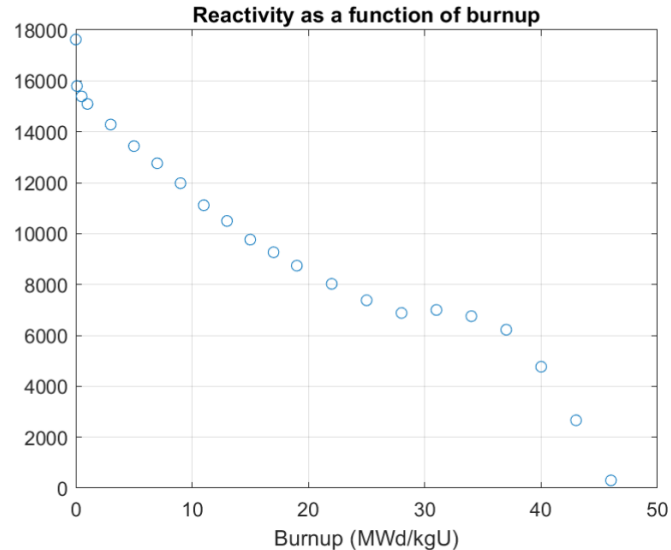


Poisoned Rods

Neutron flux in the standard fuel, in poisoned rods and Gd capture rate

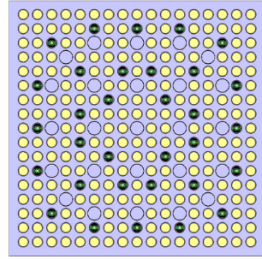


32 rods | 3D

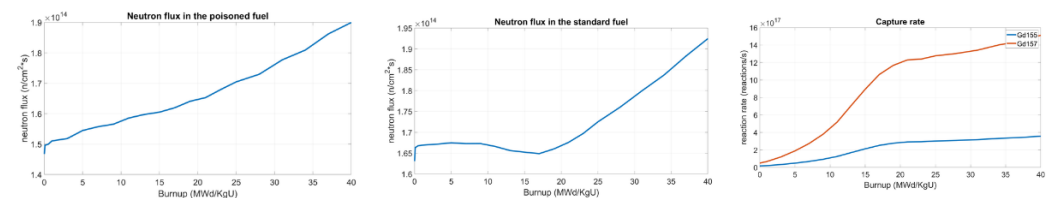
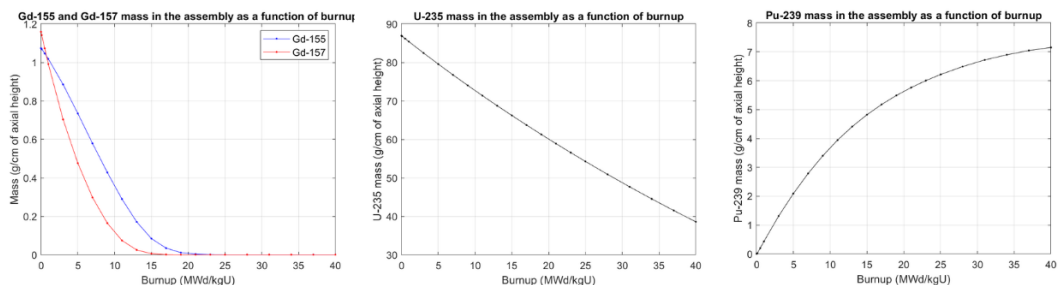
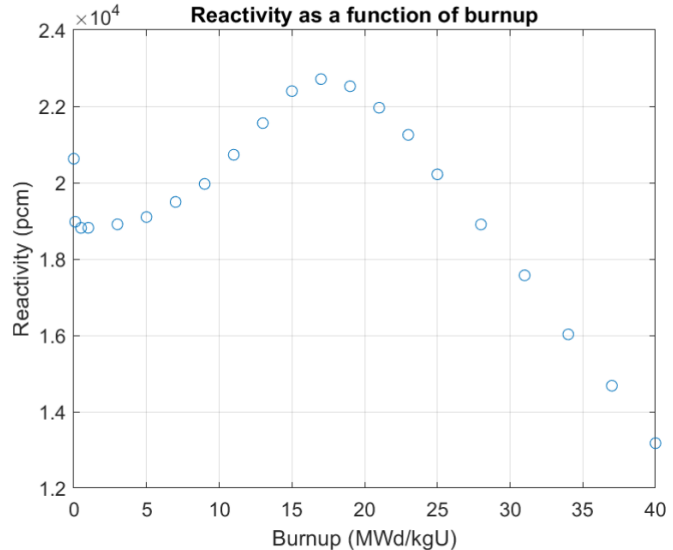


Poisoned Rods

Neutron flux in the standard fuel, in poisoned rods and Gd capture rate



32 rods | 2D



The capture rate is calculated only for Gd¹⁵⁵ and Gd¹⁵⁷ because they are the two isotopes of Gd with the largest capture cross section, as it can be seen in the following graph.

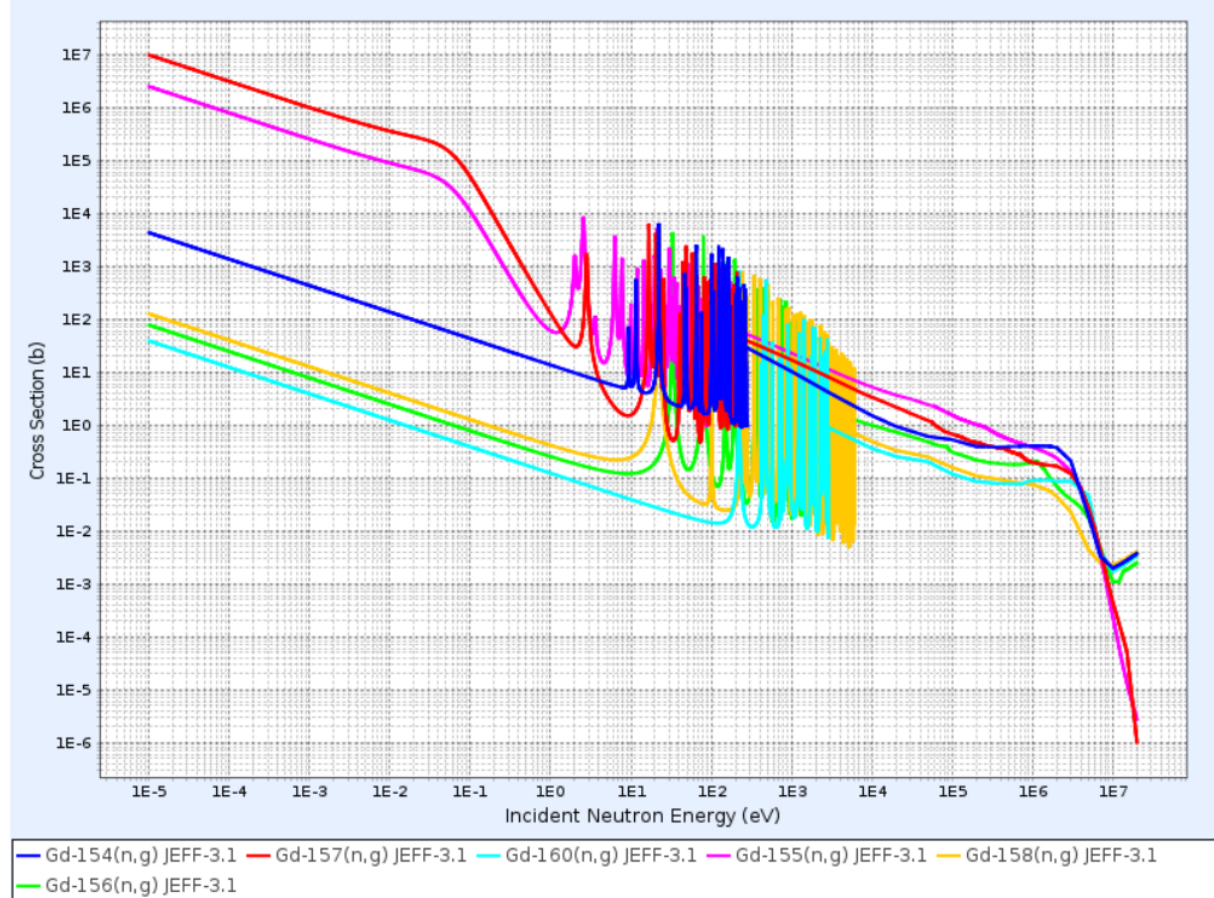


Figure A.2: Data from JEFF-3.1 nuclear data library

List of Figures

1	NUWARD reactor - section view	ii
2	NUWARD reactor - power plant	ii
3	iPWR Model - Serpent Plot	iv
2.1	Reactor 0 20 Gd rods homogeneous distribution	6
2.2	Reactor 0 20 Gd rods homogeneous distribution	7
2.3	Reactor 0 Reactivity and % Gd	8
2.4	FLEXBLUE reference Number of rods effect on 2D assembly	9
2.5	Number of rods effect on 3D assembly	9
2.6	Reactivity results for different cores	11
3.1	Reactivity as a function of the temperature of the fuel	16
3.2	Fuel Temperature Coefficient as a function of the temperature of the fuel .	16
3.3	Reactivity as a function of the temperature of the moderator	18
3.4	Moderator Temperature Coefficient as a function of the temperature of the moderator	18
3.5	Reactivity as a function of power	20
3.6	Power coefficient as a function of power	21
3.7	Reactivity as a function the of void fraction x	22
3.8	Void Coefficient as a function of the void fraction x	22
3.9	Reactivity as a function of void position	23
3.10	K_{eff} as a function of void position	23
4.1	Control rods inserted in assembly type reactor 4 section view	25
4.2	Control rods inserted in assembly type reactor 4 upper view	25
4.3	Approximated anti-reactivity insertion curve for CRs group	29
4.4	Power profile control rods fully out control rods 45 % in	29
5.1	U-235 and Pu-239 fission cross sections KAERI	32
A.1	Burnup mesh - section and axial view - BOL and EOL	35
A.2	Data from JEFF-3.1 nuclear data library	42

List of Tables

1.1	NUWARD - General Overview	2
1.2	NUWARD - Reactor Data	2
2.1	NUWARD - Core Data	5
2.2	Reactor 0 - Data	6
2.3	k_{eff} -pitch results for Reactor 0	6
2.4	Core configurations	11
3.1	Power coefficient - Input parameters	20
4.1	Cold Shutdown conditions	26
4.2	Antireactivity insertion and CR position	28
4.3	Axial offset results	29